Available online at www.sciencedirect.com
SCIENCE DIRECT
Journal of Power Sources 146 (2005) 719–722
JOURNAL OF POWER SOURCES
www.elsevier.com/locate/jpowsour

Development of high-voltage and high-capacity all-solid-state lithium secondary batteries

Yo Kobayashi *, Shiro Seki, Atsushi Yamanaka, Hajime Miyashiro, Yuichi Mita, Toru Iwahori

Central Research Institute of Electric Power Industry, 2-11-1 Iwado-kita Komae, Tokyo 201-8511, Japan

Available online 1 June 2005

Abstract

We have previously indicated that the improvement of the interface degradation between a positive electrode and an ethylene oxide-based solid polymer electrolyte (SPE) is an important problem requiring a solution for all-solid-state lithium secondary batteries. Therefore, Li_3PO_4 thin-film on $LiCoO_2$ powder was prepared by the spray coating technique. The observed Li_3PO_4 film was so thin (approximately 20 nm thick) that its contribution to the increase in interfacial resistance was small. However, it played the role of an oxidation barrier for the SPE. A [Li_3PO_4-coated $LiCoO_2$|SPE|Li] cell exhibited reversibility up to 4.6 V with a 200 mAh g^{-1} discharge capacity. The energy density of 760 mWh g^{-1} is one of the highest values obtained for all-solid-state lithium secondary batteries.

Keywords: All-solid-state lithium polymer battery; Ceramic/polymer composite electrolyte; Lithium cobalt oxide; Lithium phosphate; Oxidation barrier

1. Introduction

The conventional lithium-ion cell is widely used in portable electric devices and is now being investigated for high-power applications such as hybrid-type electric vehicles (HEVs). On the other hand, a large-scale battery system is required for use with stationary-type dispersed power sources such as polymer electrolyte fuel cell (PEFC) and photovoltaic (PV) systems. In such systems, extremely high-power is not required, but larger capacities are in demand. A solvent-free polymer lithium secondary battery is suitable for use as a stationary-use large-scale battery from the viewpoint of ultimate safety. However, combining a high-voltage positive electrode with the polymer electrolyte is difficult because the oxidation resistivity of the ethylene oxide units is poor, and therefore, the charge cutoff voltage limit of the polymer-type cell was only approximately 4 V versus Li^+/Li [1]. On the other hand, the application of high-voltage (>4.5 V) electrodes has recently been reported [2,3], and this is expected to lead to the improvement of energy density. All-solid-state batteries with high-voltage electrodes have been reported by Bates et al. [4], West et al. [5] and Whitacre et al. [6]. The electrolyte used in their studies was the so-called "LiPON" electrolyte, which could only be prepared by the sputtering method. Furthermore, the change in volume of the electrodes during charge and discharge could not be accepted in the rigid all-ceramic system, and thus, it was difficult to realize the scale-up of the battery with the use of only the LiPON-type electrolyte. Therefore, we propose a ceramic/polymer composite electrolyte in which the inorganic electrolyte is sandwiched between the positive electrode and the solid polymer electrolyte (SPE), as shown in Fig. 1. In such a ceramic/polymer composite system, the ceramic electrolyte acts as an oxidation barrier for the SPE. The SPE acts as a buffer against the volume change. We have also reported the ceramic/polymer composite-type cell with 4 V class ($LiMn_2O_4$) [7] and 5 V class ($LiNi_{0.5}Mn_{1.5}O_4$) [8] electrodes. However, the electrodes used were also thin-films because of the simple determination at the electrolyte/electrode interface. In order to achieve the scaling up of the battery, the positive electrode should be changed to powder for easy preparation and to obtain a sufficient surface area. Therefore, an appropriate procedure for the

* Corresponding author. Tel.: +81 3 3480 2111; fax: +81 3 3488 6697.
E-mail address: kobayo@criepi.denken.or.jp (Y. Kobayashi).

0378-7753/$ – see front matter © 2005 Elsevier B.V. All rights reserved.
doi:10.1016/j.jpowsour.2005.03.162

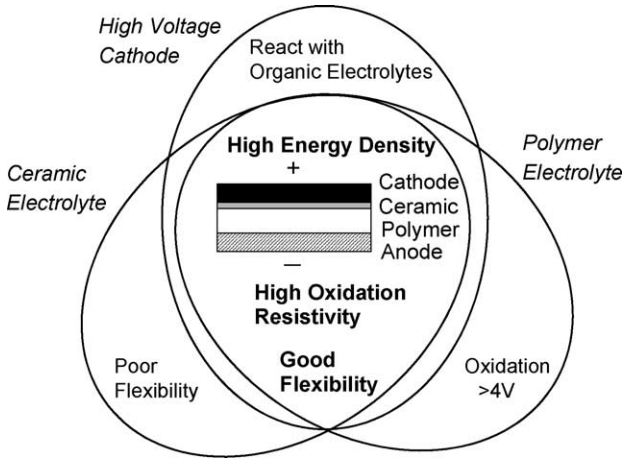

Fig. 1. A schematic of "ceramic/polymer composite concept".

coating of a ceramic electrolyte on the positive-electrode powder is needed for the scaling up of the battery. In this study, we report on thin-film ceramic electrolyte formation on powder $LiCoO_2$ by spray coating. Furthermore, we also demonstrate the possibility of a high-voltage (>4.2 V) and high-capacity (200 mAh g^{-1}) battery by combining $LiCoO_2$ with a ceramic/polymer composite electrolyte.

2. Experimental

Thin-film ceramic–electrolyte-coated $LiCoO_2$ powder was obtained by spray coating (Powrex MP-01) a precursor solution in which a 4:1 ratio of $LiNO_3$ and H_3PO_4 was dissolved in H_2O. The prepared solution was relatively Li-rich in order to avoid a Li-poor condition at the electrode surface, which might lead to the deintercalation of lithium ions from $LiCoO_2$ or the formation of impurities such as pyrophosphates during the coating process. The obtained powder was annealed at 823 K for 10 h in an O_2 flow. The formed film structure was determined by XRD analysis, SEM and TEM. The XRD data were collected in the 2θ range of 20°–110° in the step scan mode with a step width of 0.02°, and were refined using a Rietveld fitting program, RIETAN 2000 [9]. The chemical composition of the thin-film coated $LiCoO_2$ was determined by ICP. The positive electrode sheet was prepared using the mixture of coated $LiCoO_2$, acetylene black and the polymer electrolyte binder, which consisted of lithium bis(pentafluoroethylsufonyl)-amide (Li-BETI) and the polymer electrolyte, ethylene oxide *co*-2-(2-methoxy-ethoxy) ethyl glycidyl ether [P(EO/MEEGE)] (Daiso Co. Ltd.). The SPE sheet, sandwiched between the positive electrode and the negative lithium electrode, was a sheet of P(EO/MEEGE/AGE) (allyl glycidyl ether: AGE). The dissolved salt in the SPE sheet was lithium bis(trifluoromethanesufonyl)-amide (LiTFSI). The coin-type cell (CR2032) was set up in an Ar-filled glove box. The electrochemical characterization of the cell was performed using a multichannel potentiostat, Princeton Applied Research VMP2/Z. The applied ac signal for the electrochemical impedance spectroscopy (EIS) measurement was 10 mV, at a frequency between 200 kHz and 50 mHz. The charge and discharge were performed between 3.0 V and 4.6 V at 333 K. The applied constant current was 50 μA cm^{-2}, which corresponded to a rate of C/20.

3. Results and discussion

Fig. 2 shows the XRD pattern of the thin-film-coated $LiCoO_2$ with the spray coating. The formed coating material was confirmed to be Li_3PO_4 on the basis of the diffraction pattern. The observed pattern was fitted by a two-phase model, $LiCoO_2$ (hexagonal space group, *R*-3*m*) and Li_3PO_4 (orthorhombic space group, *Pmn*21). The structural parameters are given in Table 1. The parameters of noncoated $LiCoO_2$ are also shown as reference. The noncoated $LiCoO_2$ contained a trace impurity of Co_3O_4 (<1 wt%). However, the Li_3PO_4-coated $LiCoO_2$ showed no diffraction from Co_3O_4. As the coating precursor solution was relatively Li-rich, it was possible that the remnant Li compounds would react with Co_3O_4 and form $LiCoO_2$. The base $LiCoO_2$ showed no significant change in lattice parameter during the coating and post annealing process.

Fig. 3 shows the surface morphologies of Li_3PO_4-coated $LiCoO_2$. Fine Li_3PO_4 particles (approximately 100 nm ϕ) are observed on $LiCoO_2$. Some residual Li_3PO_4 particles were not used for coating, rather they accumulated. Fig. 4 shows a typical TEM cross-section of the Li_3PO_4-coated $LiCoO_2$. A uniform thin-film (approximately 20 nm thick) layer was observed on the $LiCoO_2$. Phosphorus characteristic X-rays were observed at the thin-film layer by EDX. The average thickness of Li_3PO_4 (T_{film}) is calculated using the following equation.

$$T_{film} = \frac{R_{film}}{S_{cathode} d_{film}} \quad (1)$$

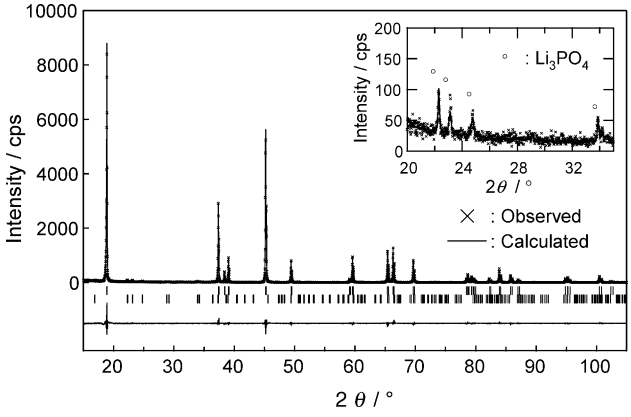

Fig. 2. The X-ray diffraction pattern for observed Li_3PO_4-coated $LiCoO_2$ (×) and the fitting result of space groups of *R*-3*m* ($LiCoO_2$) and *Pmn*21 (Li_3PO_4) (—). The inset shows the close-up of the diffractions for Li_3PO_4.

Table 1
X-ray diffraction Rietveld refinement results for Li_3PO_4-coated $LiCoO_2$

Atom	Position	x	y	z	Occupancy	B (Å^2)
Li_3PO_4-coated $LiCoO_2$: space group R-3m, a = 2.81498 (8) Å, c = 14.0479 (3) Å (*non coated $LiCoO_2$ a = 2.81536 (5) Å, c = 14.0513 (2) Å), R_I = 3.96, R_F = 2.85						
Li	3a	0.0	0.0	0.0	1.0	1.2 (2)
Co	3b	0.0	0.0	0.5	1.0	0.26 (3)
O	6c	0.0	0.0	0.2392 (2)	1.0	0.48 (6)
Li_3PO_4 on $LiCoO_2$: space group Pmn21, a = 6.115 (3) Å, b = 5.236 (3) Å, c = 4.926 (6) Å, R_I = 32.33, R_F = 23.65						
P	2a	0.0	0.816 (8)	0.0	1.0	0.5
O(1)	4b	0.217 (9)	0.673 (13)	0.908 (22)	1.0	1.0
O(2)	2a	0.0	0.101 (16)	0.914 (33)	1.0	1.0
O(3)	2a	0.5	0.175 (17)	0.909 (22)	1.0	1.0
Li(1)	4b	0.243 (40)	0.319 (49)	0.793 (39)	1.0	1.0
Li(2)	2a	0.5	0.806 (56)	1.02 (12)	1.0	1.0

R_{wp} = 17.15, R_p = 10.76, $S = R_{wp}/R_e$ = 1.30.

Here, R_{film} is the ratio of the Li_3PO_4 weight to the total weight. R_{film} (3.7 wt%) was obtained from the analysis of ICP. $S_{cathode}$ is the BET surface area of the noncoated $LiCoO_2$ (0.5 m^2 g^{-1}) and d_{film} is the theoretical density of Li_3PO_4 (2.46 g cm^{-3}) [10]. The calculated result (T_{film} = 30 nm) was reasonable, allowing for the fact that some Li_3PO_4 particles remained uncoated as shown in Fig. 3.

The Li_3PO_4 coating effect on the SPE was determined under the high-oxidation condition of $LiCoO_2$, by EIS analysis. Li_3PO_4-coated and noncoated [$LiCoO_2$|SPE|Li] cells were charged up to 4.4 V, and subjected to a constant voltage (CV). EIS measurements were performed every hour and the changes in the spectra were determined. Details of the procedure are discussed in reference [11]. Fig. 5 shows the EIS results obtained 1 h and 50 h after 4.4 V CV charging. The left and right semicircles are assigned respectively to the Li/SPE interface and $LiCoO_2$/SPE interface [11]. The EIS spectra of the coated and noncoated cell showed that they had similar profiles after the period of 1 h as shown Fig. 5(a). Although Li_3PO_4 was a relatively poor ionic conductor [12], no significant increase in interfacial resistance was observed because of the thin-film formation and because of the large surface area of the positive-electrode powder. The right-hand semicircle ($LiCoO_2$/SPE) became larger than the left-side one (Li/SPE) as holding time increased. However, the growth of the semicircle was restrained in the Li_3PO_4-coated $LiCoO_2$ system in comparison with the noncoated one. In general, the SPE is thought to be oxidized in this voltage region (4.4 V). It is notable that Li_3PO_4-coated $LiCoO_2$ showed a marked increase in interfacial resistance at the $LiCoO_2$/SPE interface in the high-voltage region.

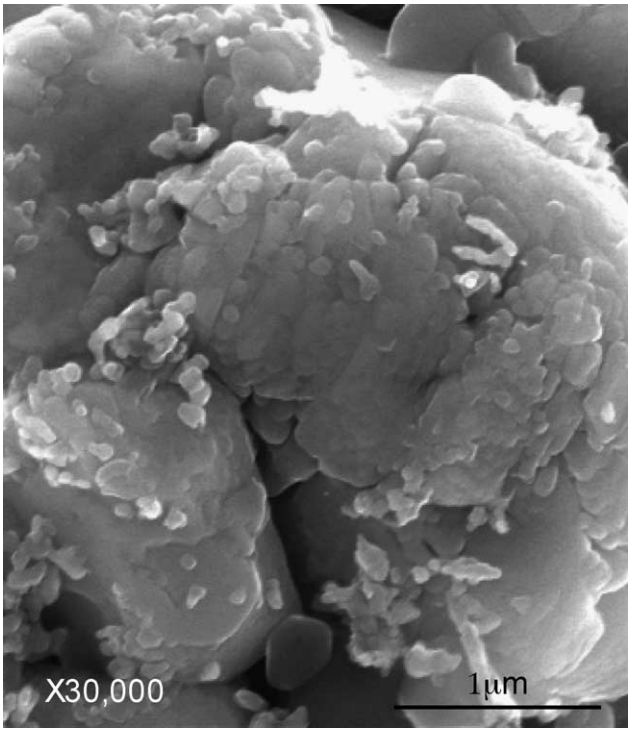

Fig. 3. SEM image of Li_3PO_4-coated $LiCoO_2$.

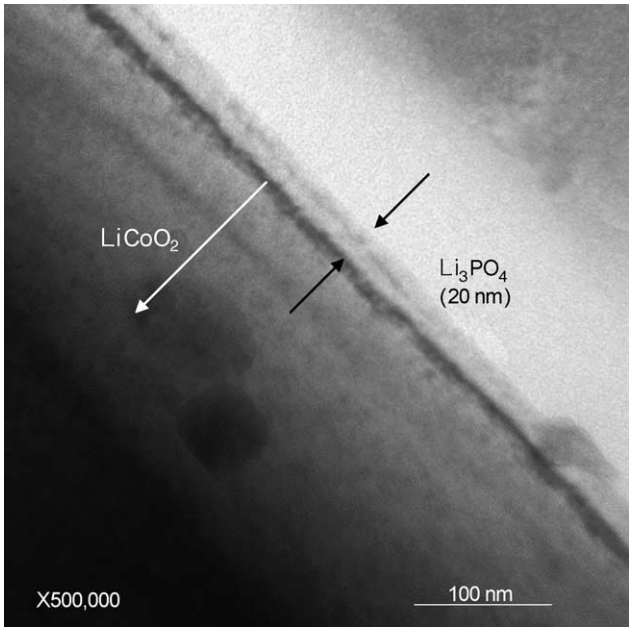

Fig. 4. TEM cross-section image of Li_3PO_4-coated $LiCoO_2$.

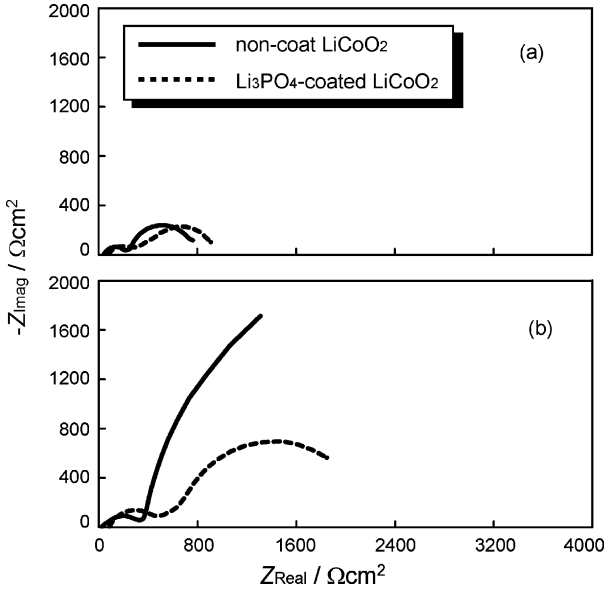

Fig. 5. The time dependences of impedance spectra of noncoated and Li_3PO_4-coated $LiCoO_2$ after a period of (a) 1 h and (b) 50 h.

The charge and discharge voltage profiles of the three initial cycles are shown in Fig. 6. The initial discharge capacity of the Li_3PO_4-coated $LiCoO_2$ was observed to be approximately 200 mAh g^{-1} and the following reversibility was fairly good. On the other hand, the noncoated $LiCoO_2$ could not attain 4.6 V during the initial charge because of the oxidation decomposition at $LiCoO_2$ and the polymer interface. Thus, we confirmed that thin-film Li_3PO_4 plays the role of the oxidation barrier for the SPE, and also of the lithium ionic conductor between $LiCoO_2$ and the SPE. The highest reported charge voltage was that reported previously by Iwamoto et al., which was 4.6 V in a sulfide-based glass electrolyte in the $LiCoO_2$ series [13]. However, the operation condition during charging was very high-rate, which involved a large polarization. The reversibility up to 4.6 V in the $LiCoO_2$ system is one of the highest reported values for all-solid-state batteries. On the other hand, a 200 mAh g^{-1} reversible capacity with SPE was also reported by Baudry et al. [14]. However, the positive electrode they used was vanadium oxide and the average discharge voltage was 2.5 V. The obtained average discharge voltage of our system was 3.81 V at the first discharge. Therefore, the total energy density of our result (760 mWh g^{-1}) is also one of the highest values reported for all-solid-state lithium secondary batteries.

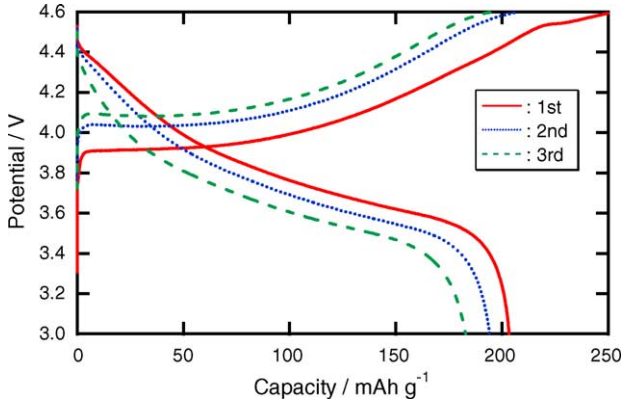

Fig. 6. Charge and discharge profiles of Li_3PO_4-coated $LiCoO_2$ (4.6 V/3.0 V cutoff, 50 μA cm^{-2}, 333 K).

4. Conclusion

Li_3PO_4 thin-film coating on $LiCoO_2$ was obtained by spray coating, and it was found that thin-film coating was possible without causing significant degradation of $LiCoO_2$. Although the observed Li_3PO_4 film was very thin (approximately 20 nm thick) the film played the important role of an oxidation barrier for the ethylene oxide-based solid polymer electrolyte. The [Li_3PO_4-coated $LiCoO_2$|SPE|Li] cell exhibited reversibility up to 4.6 V with 200 mAh g^{-1} and 760 mWh g^{-1} discharge capacities. Therefore, we believe that the ceramic/polymer composite electrolyte will enable the development of a high-energy-density battery system with sufficient safety.

Acknowledgements

The authors thank Daiso Co. Ltd. and Powrex Co. for their technical support in our research.

References

[1] A. Nishimoto, K. Agehara, K. Furuya, T. Watanabe, M. Watanabe, Macromolecules 32 (1999) 1541.
[2] H. Kawai, M. Nagata, H. Tsukamoto, A.R. West, J. Mater. Chem. 8 (1998) 837.
[3] Z. Wang, C. Wu, L. Liu, F. Wu, L. Chen, X. Huang, J. Electrochem. Soc. 149 (4) (2002) 466.
[4] J.B. Bates, D. Lubben, N.J. Dudney, F.X. Hart, J. Electrochem. Soc. 142 (9) (1995) L149.
[5] W.C. West, J.F. Whitacre, B.V. Ratnakumar, J. Electrochem. Soc. 150 (12) (2003) A1660.
[6] J.F. Whitacre, W.C. West, B.V. Ratnakumar, J. Electrochem. Soc. 150 (12) (2003) A1676.
[7] Y. Kobayashi, H. Miyashiro, T. Takeuchi, H. Shigemura, N. Balakrishnan, M. Tabuchi, H. Kageyama, T. Iwahori, Solid State Ionics 152–153 (2002) 137.
[8] Y. Kobayashi, H. Miyashiro, K. Takei, H. Shigemura, M. Tabuchi, H. Kageyama, T. Iwahori, J. Electrochem. Soc. 150 (12) (2003) A1586.
[9] F. Izumi, T. Ikeda, Mater. Sci. Forum 198 (2000) 321.
[10] C. Keffer, A.D. Mighell, F. Mauer, H. Swanson, S. Block, Inorg. Chem. 6 (1967) 119.
[11] S. Seki, Y. Kobayashi, H. Miyashiro, A. Yamanaka, Y. Mita, T. Iwahori, J. Power Sources 146 (2005) 741–744.
[12] Yu Xiaohua, J.B. Bates, G.E. Jellison Jr., F.X. Hart, J. Electrochem. Soc. 144 (2) (1997) 524.
[13] K. Iwamoto, N. Aotani, K. Takada, S. Kondo, Solid State Ionics 79 (1995) 288.
[14] P. Baudry, S. Lascaud, H. Majastre, D. Bloch, J. Power Sources 68 (1997) 432.